UCSF
UC San Francisco Previously Published Works

Title
Reduced PDZ Interactions of Rescued ΔF508CFTR Increases Its Cell Surface Mobility*

Permalink
https://escholarship.org/uc/item/4rk145k4

Journal
Journal of Biological Chemistry, 287(52)

ISSN
0021-9258

Authors
Valentine, Cathleen D
Lukacs, Gergely L
Verkman, Alan S
et al.

Publication Date
2012-12-01

DOI
10.1074/jbc.m112.421172

Peer reviewed

eScholarship.org Powered by the California Digital Library
University of California

THE JOURNAL OF BIOLOGICAL CHEMISTRY VOL. 287, NO. 52, pp. 43630–43638, December 21, 2012
© 2012 by The American Society for Biochemistry and Molecular Biology, Inc. Published in the U.S.A.

Reduced PDZ Interactions of Rescued ΔF508CFTR Increases Its Cell Surface Mobility*[S]

Received for publication, September 20, 2012, and in revised form, October 12, 2012 Published, JBC Papers in Press, October 31, 2012, DOI 10.1074/jbc.M112.421172

Cathleen D. Valentine[‡], Gergely L. Lukacs[§], Alan S. Verkman[‡], and Peter M. Haggie[‡1]

From the [‡]Department of Medicine, University of California, San Francisco, California 94143-0521 and the [§]Department of Physiology and Groupe de Recherche Axé sur la Structure des Protéine (GRASP), McGill University, Montreal, Quebec H3G 1Y6, Canada

Background: Phenylalanine 508 deletion from CFTR (ΔF508CFTR) is the most common cause of CF.
Results: Diffusional mobility of surface ΔF508CFTR is greater than that of wild type CFTR, irrespective of ΔF508CFTR rescue mechanism.
Conclusion: Defective ΔF508CFTR-PDZ interactions result in greater ΔF508CFTR diffusion and could contribute to its enhanced internalization.
Significance: Restoring ΔF508CFTR-scaffold interaction may have therapeutic benefit.

Deletion of phenylalanine 508 (ΔF508) in the cystic fibrosis transmembrane conductance regulator (CFTR) plasma membrane chloride channel is the most common cause of cystic fibrosis (CF). Though several maneuvers can rescue endoplasmic reticulum-retained ΔF508CFTR and promote its trafficking to the plasma membrane, rescued ΔF508CFTR remains susceptible to quality control mechanisms that lead to accelerated endocytosis, ubiquitination, and lysosomal degradation. To investigate the role of scaffold protein interactions in rescued ΔF508CFTR surface instability, the plasma membrane mobility of ΔF508CFTR was measured in live cells by quantum dot single particle tracking. Following rescue by low temperature, chemical correctors, thapsigargin, or overexpression of GRASP55, ΔF508CFTR diffusion was more rapid than that of wild-type CFTR because of reduced interactions with PDZ domain-containing scaffold proteins. Knock-down of the plasma membrane quality control proteins CHIP and Hsc70 partially restored ΔF508CFTR-scaffold association. Quantitative comparisons of CFTR cell surface diffusion and endocytosis kinetics suggested an association between reduced scaffold binding and CFTR internalization. Our surface diffusion measurements in live cells indicate defective scaffold interactions of rescued ΔF508CFTR at the cell surface, which may contribute to its defective peripheral processing.

The cystic fibrosis transmembrane conductance regulator (CFTR)[2] is a cAMP-regulated chloride/bicarbonate channel predominantly expressed at the apical plasma membrane of epithelial cells in the airways, pancreas, kidney, testes, and gastrointestinal tract (1, 2). Loss-of-function mutations in the *CFTR* gene cause cystic fibrosis (CF) (1). The most common CF-causing mutation is deletion of phenylalanine at position 508 (ΔF508) of CFTR, which causes its retention in the endoplasmic reticulum (ER) and ubiquitin (Ub)-dependent proteasomal degradation (3, 4).

Cell membrane chloride conductance can be partially restored by maneuvers that correct (or rescue) ΔF508CFTR biosynthetic processing, promoting its exit from the ER and targeting to the cell surface. Experimental rescue maneuvers include permissive temperature (<30 °C), alteration of ER Ca^{2+}, and activation of alternative ER export pathways (5–10). Several classes of drug-like small molecules also restore ΔF508CFTR processing and function (11–13). However, after correction, plasma membrane stability of ΔF508CFTR is reduced compared with that of native, wild-type (wt) CFTR. Incubation of low-temperature rescued (r)ΔF508CFTR at physiological temperature causes conformational destabilization, with ubiquitination, accelerated endocytosis, and lysosomal degradation (14, 15). Similar data have been obtained with rescue by chemical correctors (11, 12, 16).

Residues at the C terminus of CFTR (DTRL) form a class I PDZ (postsynaptic density protein 95/discs large/zonula occludens-1) binding domain that associates with various PDZ domain-containing scaffold proteins including EBP50 (ezrin-binding phosphoprotein of 50 kDa), CAL (CFTR-associated ligand), members of the GRASP (Golgi reassembly stacking protein) family and Shank2 (SH3 and multiple ankyrin repeat domains protein 2); however, the role of CFTR-PDZ interactions remains incompletely resolved (17). The CFTR PDZ-binding domain was originally reported to mediate apical polarization (18); however, these findings were challenged (19). Swiatecka-Urban *et al.* (20) reported that deletion of the CFTR PDZ-binding domain decreased CFTR stability by reducing recycling rates but not endocytosis. In contrast, Lukacs and co-workers (19, 21) reported that short C-terminal deletions from CFTR did not alter protein stability, whereas deletion of

* This study was supported, in whole or in part, by National Institutes of Health Grants DK081355 (to P. M. H.), DK075302 (to G. L. L.), EB000415 (to A. S. V.), a Research Development Program grant from the Cystic Fibrosis Foundation (to P. M. H. and A. S. V.), and a grant from the Canadian Institute of Health Research (to G. L. L.).
[S] This article contains supplemental Fig. S1.
[1] To whom correspondence should be addressed: 1246 HSE, 513 Parnassus Ave, University of California, San Francisco, San Francisco, CA, 94143-0521. Tel.: 415-476-8530; Fax: 415-665-3847; E-mail: peter.haggie@ucsf.edu.
[2] The abbreviations used are: CFTR, CF transmembrane conductance regulator; CF, cystic fibrosis; PDZ, postsynaptic density protein 95/discs large/zonula occludens-1; PPQC, peripheral protein quality control; SPT, single particle tracking; AMPAR, α-amino-3-hydroxy-5-methyl-4-isoxazolepropionic acid receptor.

large regions (>50 amino acids) did increase CFTR turnover. In the Golgi, modulation of the function or abundance of PDZ-domain containing proteins has been shown to correct ΔF508CFTR trafficking (10, 22, 23). Similarly, EBP50 has been implicated in rΔF508CFTR biosynthetic processing. Knockdown of EBP50 in immortalized airway epithelial cells has been reported to reduce the surface stability of both wtCFTR and low-temperature rΔF508CFTR (24). In contrast, overexpression of EBP50 was found to rescue ΔF508CFTR in CFBE41o- cells by a mechanism that involved cytoskeletal reorganization through EBP50-RhoA-Rho kinase-ezrin interactions (25, 26).

Using single particle tracking (SPT) in live cells, we previously demonstrated that PDZ interactions mediate the formation of a CFTR-containing macromolecular complex at the cell surface (Fig. 1*A*, *top* and Refs. 27, 28). SPT offers advantages over ensemble-averaged biophysical approaches used to study protein interactions in live cells. SPT provides information simultaneous on many cell surface proteins at exogenous expression levels with nanometer spatial and millisecond temporal resolution, allowing quantification of complex diffusive behaviors of protein subpopulations (29). In comparison to biochemical approaches involving cell disruption and detergent solubilization, SPT can detect weak or transient interactions in live cells.

In this study, we used SPT to test the hypothesis that ΔF508CFTR-PDZ protein interactions are reduced compared with those of wtCFTR. We found increased cell surface mobility of rΔF508CFTR compared with that of wtCFTR, which were found to involve reduced PDZ-interactions and elements of the peripheral quality control machinery. Disruption of CFTR-PDZ interactions enhanced endocytosis of wild type and ΔF508CFTR, suggesting a possible role of reduced PDZ interactions in the accelerated internalization of ΔF508CFTR.

EXPERIMENTAL PROCEDURES

Antibodies, siRNA, Additional Reagents, and cDNA Constructs—Antibodies and siGENOME SMARTpool siRNA were used as previously described (15). VX-809 was purchased from Selleckchem. CoPo-22 (13) was provided by the UCSF Cystic Fibrosis Foundation Research and Development Program. Plasmid expression vectors encoding human wt- or ΔF508CFTR with triplet HA tags have been described and characterized previously (11, 15, 27). Additional CFTR constructs containing an external triplet FLAG tag were generated in pcDNA3.1 using engineered human CFTR cDNA (30); constructs were characterized functionally using a halide sensitive YFP assay as previously described (30). The C-terminal domain of CFTR with (residues 1432–1480) and without the PDZ-binding domain (residues 1432–1476) were amplified by PCR and ligated into pmCherry-C1. Plasmids encoding Myc-tagged human CHIP and CHIP-K30A were previously described (15). GFP-GRASP55 encoding plasmid was purchased from OriGene.

Cell Culture, Transfection, and Rescue of Δ508-CFTR Processing—HeLa cell lines stably expressing 3HA-tagged CFTR constructs were previously described (15). An MDCK type II cell line expressing 3HA-tagged wtCFTR was previously described (27), and ΔF508CFTR-expressing cells were generated in an analogous manner. Untransfeceted COS-7 and MDCK cells were obtained from the UCSF Cell Culture Facility. For all microscopy, cells were cultured on 18-mm coverslips in 12-well cell culture plates for 2–4 days prior to experiments. Cells were transiently transfected using Lipofectamine 2000 (Invitrogen) 2–3 days prior to experiments. Low temperature rescue of ΔF508CFTR was performed by incubating cells at 27 °C for 24–30 h; as necessary, subsequent thermal unfolding was performed by incubation of cells for an additional 1–2 h at 37 °C (15). The following pharmacological maneuvers were used to correct ΔF508CFTR trafficking: 3 μM VX-809 for 24 h (12), 10 μM CoPo-22 for 24 h (13), and 1 μM thapsigargin for 2 h (10).

Single Particle Tracking and Data Analysis—Qdot-labeling, SPT data collection, and analysis was performed essentially as described in prior studies (27, 28, 31). Data were collected with a Nikon 100×/N.A 1.3 objective. Datasets were compiled from 110–788 trajectories (average of 215 trajectories per maneuver) obtained from multiple cells on different days. Given that CFTR is endocytosed, experiments were performed within 3–5 min of labeling to reduce errors associated with inclusion of data derived from endocytosed CFTR molecules (which is assumed to be <10% in all datasets). Statistical analysis of SPT data were performed using the Kolmogorov-Smirnov test (31, 32).

Determination of CFTR Surface Density, Stability, and Endocytosis Rates—Epitope-tagged CFTR surface density and endocytic rates were determined essentially as described in a prior study (15). Cell surface density of epitope-tagged CFTR variants was measured by labeling surface CFTR at 4 °C with primary antibody (anti-HA or anti-FLAG) followed by: (i) a secondary antibody conjugated to fluorophore for image-based detection (after fixation), or (ii) horseradish peroxidase conjugated secondary antibody and Amplex Red (Invitrogen) for quantification in an ELISA format. Relative ΔF508CFTR surface density presented in Fig. 4 is the normalized difference in surface density before and after incubation at 37 °C for 2 h. To determine endocytic rates for CFTR variants, cells were labeled with primary antibody and incubated at 37 °C for 0 or 10 min prior to labeling with secondary antibody to determine CFTR surface density. Nonspecific antibody labeling was assessed using non-transfected cells. Control experiments in HeLa cells expressing 3HA-tagged CFTR verified that imaging and Amplex Red-based analysis gave equivalent results. Datasets are presented as mean ± S.E. from 3–8 independent experiments. For Amplex Red, individual measurements were performed using 6–8 parallel samples and normalized to protein content; for image-based analysis, cell surface CFTR density measurements were performed on >30 cells per data set. Statistical analysis was by *t* test.

RESULTS

Increased Cell Surface Diffusion of rΔF508CFTR Compared with wtCFTR—Initial studies were done using HeLa cells expressing CFTR constructs containing triplet hemagglutinin tags (CFTR3HA) engineered into the fourth external loop region; these cells were used previously to characterize and identify cellular components involved in rΔF508CFTR processing (15). For surface mobility measurements using SPT, cell

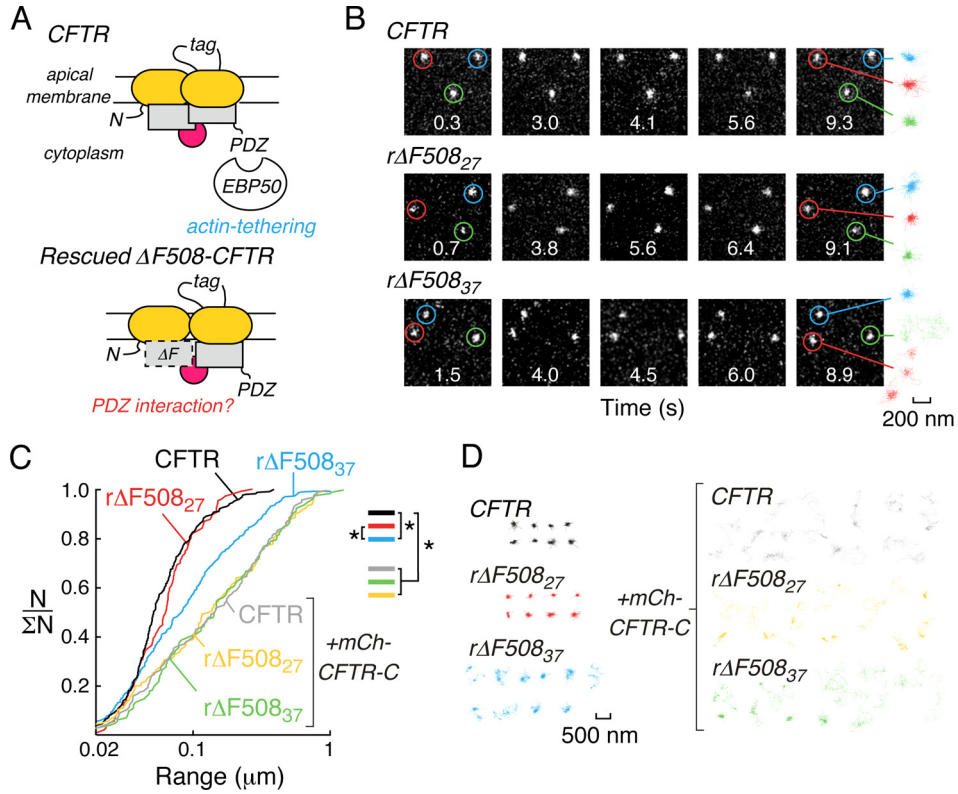

FIGURE 1. **Single-particle tracking of wild-type and low-temperature rescued (r)ΔF508CFTR in HeLa cells.** *A*, C-terminal PDZ interactions tether wtCFTR to actin (*top*) but their role in rΔF508CFTR plasma membrane stability is unknown (*bottom*). *B*, individual frames from SPT image sequences acquired at 30 fps for Qdot-labeled wtCFTR (*top*), rΔF508CFTR immediately after low temperature correction (rΔF508$_{27}$, *middle*) and rΔF508CFTR after low temperature correction and subsequent incubation at 37 °C for 2 h (rΔF508$_{37}$, *bottom*). Image acquisition time is given in each frame and highlighted exemplar trajectories are shown for each condition (*right*, 200 nm scale bar refers to all trajectories). Images are 6.4 × 6.4 μm. *C*, cumulative distribution plots for wtCFTR (*black*), rΔF508$_{27}$ (*red*), and rΔF508$_{37}$ (*blue*) under control conditions, and for wtCFTR (*gray*), rΔF508$_{27}$ (*orange*), and rΔF508$_{37}$ (*green*) when expressed with high levels of the CFTR C-terminal region (fused to mCherry, mCh-CFTR-C), which results in mobilization of CFTR. Statistically significant differences in populations are shown (*, $p <$ 0.001). N/ΣN is the normalized cumulative probability distribution where 1 represents the complete population of SPT data. SPT data were derived from 110–316 trajectories. *D*, color-coded SPT trajectories for each condition shown in Fig. 1*C* (500 nm scale bar refers to all trajectories).

surface CFTR was selectively labeled by sequential incubation with low concentrations of anti-HA antibody, secondary biotin-conjugated Fab fragment, and streptavidin-conjugated Qdots (emission 655 nm). As in prior studies (27, 31), Qdot labeling specificity was confirmed by absence of Qdot labeling when primary antibody or secondary Fab fragment were omitted, or when ΔF508CFTR was not rescued (data not shown). Diffusion of Qdot-labeled CFTR was measured at 37 °C by analysis of image sequences acquired at 30 Hz over 10 s (Fig. 1*B*). Mobility of wtCFTR was highly confined (Fig. 1*B*, *top*), as found previously for wtCFTR expressed at endogenous levels in multiple cell types, including human airway epithelial cells (27, 28). Immediately following low temperature rescue, where rΔF508CFTR plasma membrane stability, endocytosis and ubiquitination are similar to that of wtCFTR (15), the diffusion (measured at 37 °C) of rΔF508CFTR (rΔF508CFTR$_{27}$) was also similar to that of wtCFTR (Fig. 1*B*, *middle*). However, thermal unfolding of rΔF508CFTR by 2 h of incubation at 37 °C (rΔF508CFTR$_{37}$), which causes accelerated endocytosis (~2-fold), enhanced ubiquitination and an overall reduction in cells surface rΔF508CFTR levels (15), produced an increase in mobility (Fig. 1*B*, *bottom*). Trajectories generated from analysis of multiple image sequences (Fig. 1, *B*, *right* and *D*) were summarized as cumulative probability distributions of particle range at 3 s. Fig. 1*C* shows significantly greater range for rΔF508CFTR$_{37}$ diffusion (*blue*) in comparison to wtCFTR (*black*) or rΔF508CFTR$_{27}$ (*red*, see Fig. 1*D* for representative trajectories). Diffusion of wtCFTR was not altered under the same culture conditions used to rescue and thermally unfold ΔF508CFTR (supplemental Fig. S1*A*).

We previously established that confined diffusion of wtCFTR in live cells is dependent on its C terminus PDZ binding motif, PDZ domain containing scaffold proteins, and coupling to the actin cytoskeleton via ezrin (27). This finding is consistent with *in vitro* protein-protein interaction data suggesting the involvement of wtCFTR in a cell surface macromolecular complex. Here, to investigate the involvement of PDZ interactions in rΔF508CFTR confinement in live cells, a chimeric protein consisting of the C terminus of CFTR (residues 1432–1480, which does not contain the endocytic motifs ^{1413}FLVI, ^{1424}YDSI, and ^{1430}LL) fused to mCherry (mCh-CFTR-C) was expressed to compete with CFTR for attachment to PDZ domain proteins. As expected from our previous data (27), mCh-CFTR-C expression greatly increased wtCFTR diffusion (Fig. 1, *C* and *D*, *gray*). Low-temperature corrected ΔF508CFTR has been demonstrated to interact with EBP50 (24) and mCh-CFTR-C also increased the diffusion of rΔF508CFTR$_{27}$ (Fig. 1, *C* and *D*, *orange*) and rΔF508CFTR$_{37}$ (Fig. 1, *C* and *D*, *green*) to the same degree as wtCFTR, suggesting that PDZ interactions contribute to the confinement of cell surface ΔF508CFTR. As previously

demonstrated for wtCFTR (27), expression of a CFTR C-terminal fusion protein that lacked the PDZ-binding motif (mCh-CFTR-C-ΔPDZ) did not alter the diffusion of wtCFTR, ΔF508CFTR$_{27}$, and ΔF508CFTR$_{37}$ in Hela cells (supplemental Fig. S1*B*). These findings show in live cells that interactions with PDZ domain-containing proteins contribute to the tethering of wt and low-temperature rescued ΔF508CFTR, but that interactions between rΔF508CFTR$_{37}$ and PDZ domain-containing proteins are reduced compared with wtCFTR or rΔF508CFTR$_{27}$.

CFTR diffusion was measured in additional cell types and with transiently transfected CFTR constructs to verify the robustness of observations made in HeLa cell lines. In MDCK cell lines stably expressing CFTR3HA constructs, incubation of ΔF508CFTR-expressing cells at 27 °C increased ΔF508CFTR cell surface density to a level ~6-fold reduced compared with wtCFTR (supplemental Fig. S1*C*). As predicted from prior studies in different cell types (14, 15), incubation at 37 °C for 1 h to thermally denature rΔF508CFTR produced an ~50% decrease in plasma membrane rΔF508CFTR density (Fig. 2*A*, *left*) and an ~2-fold increase in endocytosis compared with wtCFTR; however, ΔF508CFTR internalization was similar to wtCFTR immediately after rescue (Fig. 2*A*, *right*).

SPT analysis of CFTR diffusion in MDCK cell lines showed highly confined diffusion of wtCFTR (*black*) and rΔF508CFTR$_{27}$ (*red*, Fig. 2*B*); however, incubation for 1 h at 37 °C increased rΔF508CFTR diffusion as seen in individual trajectories (*blue*) and cumulative probability distributions (Fig. 2*C*, *black* and *blue*). The diffusion of wtCFTR and rΔF508CFTR$_{37}$ were significantly increased by expression of mCh-CFTR-C (Fig. 2*C*, *gray* and *green*). A comparable increase in channel diffusion was seen with deletion of the C-terminal PDZ-binding motif of CFTR (CFTRΔPDZ, Fig. 2*C*, *pink*), suggesting that expression of mCh-CFTR-C mobilizes wt and rΔF508CFTR to the same degree as deletion of the PDZ-binding motif. In control experiments, mCh-CFTR-C-ΔPDZ did not alter the diffusion of wtCFTR (Fig. 5*C*), rΔF508CFTR$_{27}$ or rΔF508CFTR$_{37}$ (supplemental Fig. S1*D*), verifying the involvement of PDZ-domain interactions in confinement of wtCFTR, rΔF508CFTR$_{27}$, and rΔF508CFTR$_{37}$. The smooth shape of cumulative probability distributions suggested the absence of distinct CFTR subpopulations with different mobilities. As such, data were summarized in bar graph format (Fig. 2*D*), showing median (*blue*) and inter-quartile (25th to 75th percentiles, *red*) range values. As described above, data from MDCK cell lines (Fig. 2*D*) shows significantly different diffusion of rΔF508CFTR$_{37}$ *versus* wtCFTR or rΔF508CFTR$_{27}$ (*bars 1–3*), and increased CFTR diffusion upon disruption of PDZ interactions (*bars 3–6*).

CFTR diffusion was further studied in COS-7 fibroblasts that were transiently transfected to express CFTR constructs containing external FLAG epitopes (CFTR3FLAG). As expected, surface density decreased and endocytosis increased after 37 °C incubation of low temperature corrected ΔF508CFTR (Fig. 2*E*). The diffusion of wtCFTR and rΔF508CFTR$_{27}$ were similar in COS-7 cells, whereas incubation of rΔF508CFTR-expressing cells at 37 °C increased diffusion by ~30% (Fig. 2*F*, *bars 1–3*). Deletion of the PDZ binding motif from wtCFTR increased

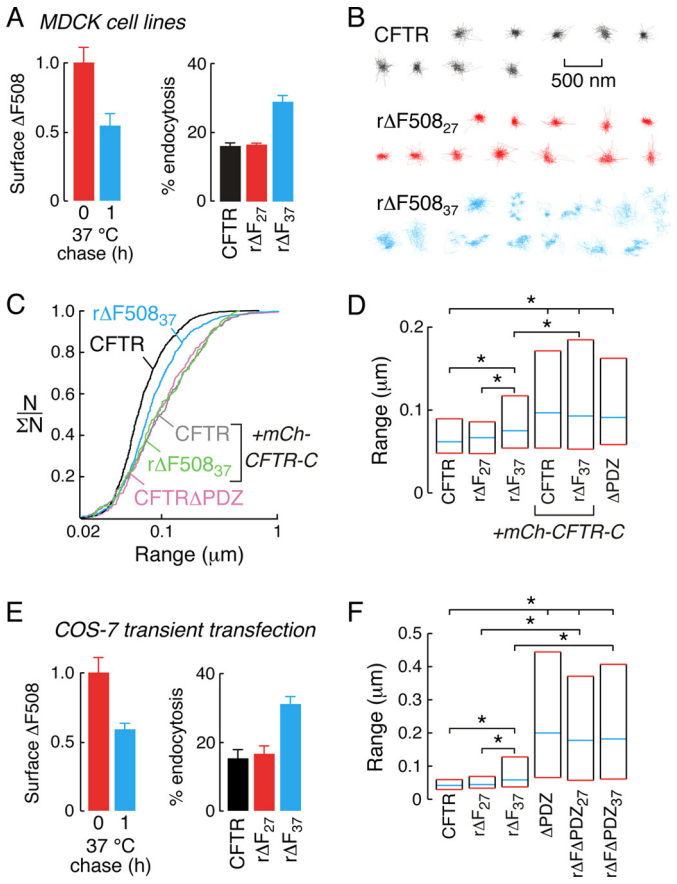

FIGURE 2. **Increased diffusion of rΔF508CFTR in MDCK cell lines and transiently transfected COS-7 cells.** *A*, low temperature corrected ΔF508CFTR surface density (*left*) and endocytic rates (*right*) in MDCK cell lines immediately after rescue (*red*) and after 1 h 37 °C incubation (*blue*). *B*, example trajectories of wtCFTR (*black*), rΔF508$_{27}$, (*red*), and rΔF508$_{37}$, (*blue*) diffusion in MDCK cell lines. *C*, cumulative distribution curves for MDCK cell lines expressing wtCFTR (*black*), rΔF508$_{37}$ (*blue*), or CFTRΔPDZ (*pink*) and co-expressing mCh-CFTR-C with wtCFTR (*gray*) or rΔF508$_{37}$, (*green*). *D*, summary graph representing median (*blue lines*) and interquartile (*red lines*) range values for the diffusion of wtCFTR, rΔF508CFTR and CFTRΔPDZ-expressing MDCK cell lines. As indicated, mCh-CFTR-C was also expressed (*bars 4* and *5*). *E*, surface levels (*left*) and endocytic rates (*right*) of low temperature corrected 3FLAG-tagged ΔF508CFTR in transiently transfected COS-7 cells immediately after rescue (*red*) and after 37 °C incubation (*blue*). *F*, summary graphs of diffusive range for 3FLAG-tagged wtCFTR, ΔF508CFTR, CFTRΔPDZ, and ΔF508CFTRΔPDZ expressing COS-7 cells. In *panels D* and *F*, statistically significant differences in populations are shown (*, $p < 0.001$). SPT data for MDCK cells was derived from 113–788 trajectories and for COS-7 cells from 140–252 trajectories. Data for CFTR surface density and endocytic rates are mean ± S.E. for 3–8 independent experiments.

diffusion (Fig. 2*F*, *bar 4*), as did deletion from ΔF508CFTR following low temperature rescue (ΔFΔPDZ$_{27}$) and subsequently incubated at 37 °C (ΔFΔPDZ$_{37}$) (Fig. 2*F*, *bars 5* and *6*). The magnitude of the effect on diffusion of PDZ-domain deletion varied for wtCFTR and rΔF508CFTR in different cell types; however, this difference likely reflects differences in plasma membrane properties as MDCK cells have been shown to reduce the diffusion of inert probe molecules as compared with other cell types (33). Further, the diffusion of wt and ΔF508CFTR in the absence of PDZ interactions in both MDCK and COS-7 cells was comparable to that of AQP1, a membrane transport protein that has largely unhindered diffusion (33). These studies confirm that in different cell types ΔF508CFTR rescued by low-temperature incubation interacts with PDZ

domain proteins in a similar manner as wtCFTR, but that thermal unfolding at 37 °C increases rΔF508CFTR diffusion by partially disrupting the interactions between rΔF508CFTR and PDZ domain-containing scaffold proteins.

ΔF508CFTR Diffusion Is Increased with Alternative Correction Methods—SPT experiments were done to investigate cell surface ΔF508CFTR-PDZ interactions following different correction maneuvers. Treatment of MDCK cell lines expressing CFTR3HA with 3 μM VX-809, a corrector drug in Phase II clinical trials (12, 34), for 24 h gave ΔF508CFTR cell surface levels similar to those produced by low-temperature rescue (supplemental Fig. S1*C*). SPT trajectories of ΔF508CFTR diffusion following VX-809 correction appeared less confined than those of wtCFTR under control conditions (Fig. 3*A*, *red* and *black trajectories*) and range values differed significantly (Fig. 3*B*, *bars 1* and *3*). Expression of mCh-CFTR-C increased the diffusion of VX-809-corrected ΔF508CFTR (Fig. 3*A*, *blue*) to that found for wtCFTR with mCh-CFTR-C or for CFTRΔPDZ (Fig. 3*B*, *bars 4–6*), confirming the involvement of PDZ interactions in restricting rΔF508CFTR mobility after VX-809 treatment. Control experiments verified that mCh-CFTR-C-ΔPDZ did not alter the diffusion of rΔF508CFTR corrected with VX-809 (data not shown).

Additional experiments were performed in transiently transfected MDCK cells using VX-809 to correct 3FLAG-tagged ΔF508CFTR to verify results generated in cell lines (Fig. 3, *C* and *D*). In transiently transfected MDCK cells, wtCFTR mobility was reduced when compared with VX-809 rescued ΔF508CFTR (Fig. 3*C*, *black* and *red*; and Fig. 3*D*, *bars 1* and *2*). The diffusion of cell surface ΔF508CFTR was increased by expression of mCh-CFTR-C (but not mCh-CFTR-C-ΔPDZ) or deletion of the ΔF508CFTR C-terminal PDZ-binding motif (rΔFΔPDZ) (Fig. 3, *C* and *D* and data not shown). VX-809 treatment did not alter the diffusion of wtCFTR or CFTRΔPDZ, suggesting that VX-809 does not perturb plasma membrane properties (for example see Fig. 3*B*, *bars 1* and *2*; Fig. 3*D*, *bars 5* and *6*).

The diffusion of cell surface ΔF508CFTR in MDCK cell lines was also increased compared with wtCFTR (Fig. 3*E*) following correction by thaspigargin (*black*), the small molecule corrector CoPo-22 (*red*), or transient expression of GFP-GRASP55 (*blue*; for all datasets $p < 0.001$ compared with wtCFTR, Fig. 3*F*, *top*). These treatments did not alter the diffusion of wtCFTR (Fig. 3*E*, *left* and Fig. 3*F*, *bottom*). For GRASP55-mediated ΔF508CFTR rescue, immunocytochemistry confirmed GFP-GRASP55 co-localization with the Golgi marker giantin (Fig. 3*G*). Photobleaching experiments using laser scanning confocal microscopy indicated that the diffusion of the inert membrane probe glycophosphatidylinositol-anchored GFP was not altered by each of the maneuvers used to correct ΔF508CFTR trafficking (data not shown). These studies thus demonstrate that, as found for low temperature correction, rescue by a variety of unrelated maneuvers produces cell surface ΔF508CFTR with abnormal PDZ-domain interactions relative to wtCFTR.

Components of the Peripheral Protein Quality Control System Modulate ΔF508CFTR Mobility—Experiments were performed to identify cellular components that are responsible for reduced ΔF508CFTR-PDZ interactions. Using a small interfering (si)-RNA screen, Okiyoneda *et al.* (15) previously identified constituents of the peripheral protein quality control (PPQC) system that recognize and eliminate low-temperature corrected and thermally denatured ΔF508CFTR from the cell surface. This approach identified the E3 Ub ligase CHIP (C terminus of Hsc70-interacting protein) and the chaperone Hsc70 (heat shock cognate of 70 kDa) as key determinants of $r\Delta F508CFTR_{37}$ turnover such that knockdown of either protein increased cell surface stability. Here, we tested whether altering the abundance or activity of CHIP and Hsc70 would also affect ΔF508CFTR mobility. $r\Delta F508CFTR_{37}$ diffusion was

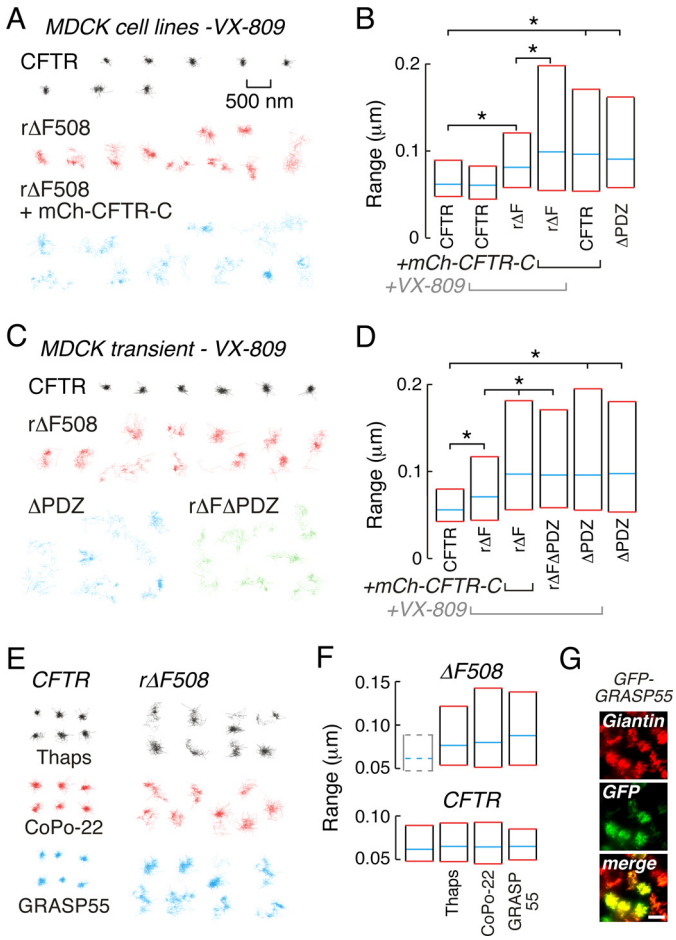

FIGURE 3. **ΔF508CFTR diffusion is increased by different correction mechanisms.** *A*, example trajectories from MDCK cell lines for wtCFTR (*black*) and ΔF508CFTR rescued by VX-809 treatment in the absence (*red*) and presence (*blue*) of mCh-CFTR-C. *B*, summary graph for wtCFTR, rΔF508CFTR and CFTRΔPDZ diffusion in VX-809-treated and control MDCK cell lines. *C*, example trajectories for MDCK cells transiently expressing 3FLAG-tagged wtCFTR (*black*), ΔF508CFTR rescued by VX-809 (*red*), CFTRΔPDZ (*blue*), and ΔF508CFTRΔPDZ rescued by VX-809 (*green*). *D*, summary graph for CFTR diffusion in VX-809-treated MDCK transiently transfected with 3FLAG-tagged CFTR constructs. *E*, example trajectories from MDCK cell lines stably expressing wtCFTR (*left*) and ΔF508CFTR (*right*) treated with thapsigargin (*black*) or CoPo-22 (*red*) or transiently expressing GFP-GRASP55 (*blue*). *F*, graphs for ΔF508CFTR (*top*) and wtCFTR (*bottom*) diffusion in MDCK cell lines treated with thapsigargin or CoPo-22 or transiently expressing GFP-GRASP55. For reference, median and interquartile values for wtCFTR diffusive range are shown by *dashed lines* (bar 1, *top*). *G*, GFP-GRASP55 is Golgi-localized by immunocytochemical analysis (scale bar, 10 μm). Scale bar in *A* (500 nm) refers to all trajectories. In *panels B* and *D*, statistically significant differences in populations are shown (*, $p < 0.001$). SPT data for MDCK cell lines was derived from 140–788 trajectories and for transiently transfected MDCK cells from 131–298 trajectories.

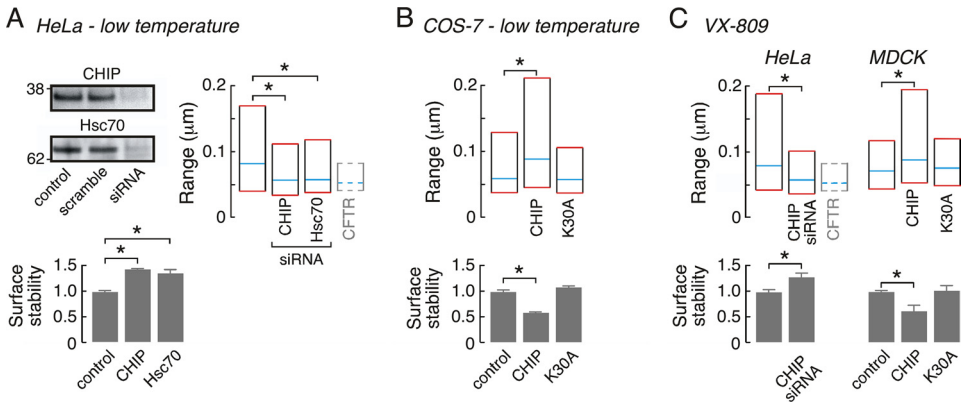

FIGURE 4. **The peripheral protein quality control (PPQC) system alters rΔF508CFTR diffusion.** *A*, effects of siRNA-mediated knockdown of CHIP or Hsc70 (*left, top*) on rΔF508CFTR$_{37}$ surface levels (*left, bottom*, values >1 represent stabilization of rΔF508CFTR$_{37}$ relative to control conditions) and diffusive range (*right*) in low temperature corrected HeLa cells. For reference, median and interquartile values for wtCFTR diffusive range are shown by dashed lines (*bar 4, right*). *B*, transient co-expression of ΔF508CFTR with CHIP but not CHIP-K30A alters rΔF508CFTR$_{37}$ diffusive range (*top*) and surface levels (*bottom*) in low temperature corrected COS-7 cells. *C*, siRNA-mediated CHIP knockdown in HeLa cells (*left*) and CHIP expression in MDCK cells (*right*) alter rΔF508CFTR diffusion (*top*) and surface levels (*bottom*) in VX-809-treated cells. For reference, median and interquartile values for wtCFTR diffusive range in HeLa cells are shown by *dashed lines* (bar 3, *left*). Statistical difference is denoted (*); for SPT data $p < 0.001$ and for surface stability data $p < 0.05$. SPT data were derived from 276–316 trajectories for low temperature corrected Hela cells, from 124–255 trajectories for COS-7 cells, from 160 and 226 trajectories for VX-809-treated Hela cells and from 162–298 trajectories for MDCK cells. Data for CFTR surface stability are mean ± S.E. for 3–8 independent experiments.

studied in HeLa cells following siRNA reduction of CHIP or Hsc70 expression by >75% (Fig. 4*A*, *left top*). In agreement with prior studies (15), knockdown of CHIP or Hsc70 increased cell surface stability of rΔF508CFTR by ~50% during subsequent 37 °C incubation (Fig. 4*A*, *left bottom*). Increasing rΔF508CFTR$_{37}$ cell surface density by CHIP or Hsc70 knockdown was also accompanied by a reduction in rΔF508CFTR$_{37}$ diffusion toward that of wtCFTR (Fig. 4*A*, *right*).

To further investigate the role of CHIP in ΔF508CFTR surface diffusion, wild type, and mutant CHIP constructs were transiently expressed in COS-7 cells. As expected based on earlier observations (15), overexpression of CHIP in COS-7 cells reduced rΔF508CFTR$_{37}$ surface stability (Fig. 4*B*, *bottom*) and also increased rΔF508CFTR$_{37}$ surface diffusion (Fig. 4*B*, *top*). CHIP binds to Hsc70 and Hsp90 (heat shock protein of 90 kDa) via an N-terminal tetratricopeptide repeat domain, and these associations are blocked in the CHIP-K30A mutant (35). Expression of CHIP-K30A in COS-7 cells did not alter rΔF508CFTR$_{37}$ diffusion or stability (Fig. 4*B*), indicating that CHIP recognition of thermally destabilized rΔF508CFTR is dependent upon Hsc70 and Hsp90. In VX-809-treated HeLa cells rΔF508CFTR diffusion was similar to that of rΔF508CFTR$_{37}$, as would be expected from prior studies in MDCK cells (Fig. 4*C*, *top left*). Further, siRNA knockdown of CHIP reduced rΔF508CFTR mobility and increased surface stability (Fig. 4*C*, *left*). CHIP expression also reduced confinement and cell surface stability of rΔF508CFTR in transiently transfected MDCK cells treated with VX-809; however, expression of CHIP-K30A did not alter diffusion or stability of VX-809-corrected rΔF508CFTR, confirming that CHIP recognition of rΔF508CFTR required Hsc70 and Hsp90 (Fig. 4*C*, *right*). In control experiments, wtCFTR mobility was not altered by CHIP knockdown in HeLa cells or CHIP overexpression in COS-7 cells; non-targeted siRNA did not alter wtCFTR or rΔF508CFTR diffusion in HeLa cells (supplemental Fig. S1*E*). These studies indicate that components of the PPQC machinery including CHIP, Hsc70 and Hsp90, contribute to the increased diffusion of cell surface ΔF508CFTR rescued by low-temperature or VX-809.

PDZ Interactions Stabilize wtCFTR at the Cell Surface—The present study indicates that reduced rΔF508CFTR surface stability is associated with increased diffusive mobility. Given that endocytosis is the initial step in reducing rΔF508CFTR surface density, an experimental strategy was developed to quantitatively investigate whether the observed increase in diffusion associated with reduced PDZ interactions of ΔF508CFTR could alter CFTR internalization rates. Our approach relied upon exogenous expression of the CFTR C terminus (mCh-CFTR-C) to increase wtCFTR mobility and thus mimic rΔF508CFTR surface dynamics (Fig. 5*A*). CFTR3HA-expressing MDCK cells were enriched for mCh-CFTR-C content by fluorescence-activated cell sorting (FACS) to generate a cell population with ~80% mCh-CFTR-C-positive cells that were readily identified in image-based assays of CFTR trafficking and surface stability (Fig. 5*B*, *left*). Expression of mCh-CFTR-C in FACS-enriched cells was relatively homogeneous (Fig. 5*B*, *right*), albeit ~40-fold less than in prior experiments that used transient transfection of the same construct. Surface expression of wtCFTR was similar in control and mCh-CFTR-C-enriched cells, suggesting that expression of exogenous CFTR C-terminal domains does not alter CFTR stability (supplemental Fig. S1*C*). This result is consistent with data from CFTR with short C-terminal deletions that show similar stability to wtCFTR (19). SPT confirmed that wtCFTR diffusion in mCh-CFTR-C-enriched cells was greater (by ~25%) than that in control cells (Fig. 5*C*, *bars 1* and *3*), and similar to that of ΔF508CFTR rescued by low-temperature or VX-809 (Fig. 5*C*, *bars 4* and *5*).

Endocytosis of wtCFTR in mCh-CFTR-C-enriched cells was increased by ~30% as compared with wtCFTR (Fig. 5*D*, *bar 1* and *3*, $p < 0.005$, ~16 *versus* 21%), suggesting that PDZ interactions stabilize CFTR at the cell surface over time scales of minutes. In support of this conclusion, deletion of the CFTR C-terminal PDZ binding domain (CFTRΔPDZ), which is expected to fully account for any PDZ-dependent component

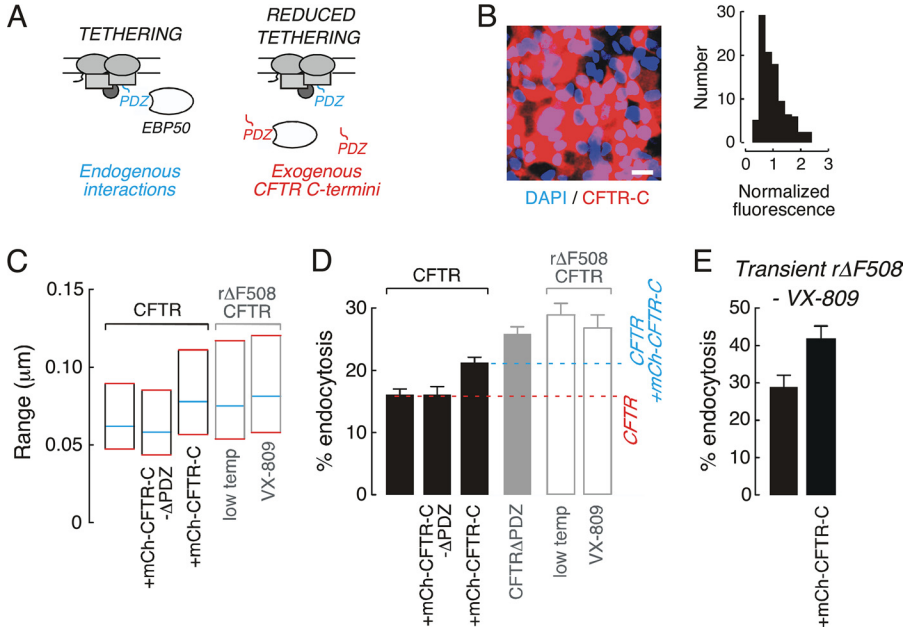

FIGURE 5. **Reduced PDZ interactions significantly enhance CFTR endocytosis rates.** *A*, schematic of experimental approach used to quantitatively relate CFTR diffusion to endocytosis. Endogenous PDZ-mediated interactions tether wtCFTR to actin (*left*) and expression of exogenous CFTR C-terminal domains reduces tethering (*right*). *B*, fluorescence image (*left*) and normalized intensity distribution of mCherry fluorescence (*right*) for CFTR3HA-expressing MDCK cells enriched for mCh-CFTR-C (scale bar, 20 μm). *C*, summary graph of CFTR diffusion in MDCK cells expressing wtCFTR (*black outlines*) and ΔF508CFTR (*gray outlines*). *D*, CFTR endocytic rates in MDCK cells expressing wtCFTR (*black*), CFTRΔPDZ (*solid gray*), and ΔF508CFTR (*gray outline*). For reference, endocytic rate of wtCFTR (*red dash line*) and of wtCFTR in cells enriched for mCh-CFTR-C expression (*blue dashed line*) are shown. *E*, endocytosis of VX-809-rescued ΔF508CFTR in transiently transfeceted MDCK cells is enhanced by high-level expression of mCh-CFTR-C. SPT data were derived from 112–788 trajectories. Data for CFTR endocytic rates are mean ± S.E. for 3–8 independent experiments.

of CFTR internalization (and increased diffusive by ~50%, Fig. 2), increased endocytosis by ~60% as compared with wtCFTR (Fig. 5*D*, *bar 4*, $p < 0.001$, ~16 *versus* 26%). Therefore, compared with wtCFTR, the percentage increase in surface diffusion and in endocytosis rate after deletion of the CFTR PDZ-binding domain or upon partial disruption of PDZ interactions to model rΔF508CFTR diffusion are in reasonable agreement. Control experiments confirmed that CFTR diffusion (Fig. 5*C*, *bar 2*) and internalization (Fig. 5*D*, *bar 2*) were not altered by enrichment of cells for expression of the PDZ binding-domain deleted CFTR C terminus (mCh-CFTR-C-ΔPDZ). Finally, in MDCK cells transiently expressing VX-809-rescued ΔF508CFTR3FLAG, co-expression of mCh-CFTR-C at high levels enhanced ΔF508CFTR internalization, confirming that PDZ interactions can also influence rΔF508CFTR endocytosis (Fig. 5*E*). These studies indicate that (i) PDZ interactions stabilize CFTR at the cell surface over time scales of minutes, and (ii) increasing the diffusion of wtCFTR to that of rΔF508CFTR is sufficient to alter internalization kinetics.

DISCUSSION

SPT provides definitive information about the motions of individual channels, receptors or lipids in the plasma membrane of live cells, which can reveal complex diffusive behaviors over extended time and distance scales (29, 36). Our prior SPT studies on wtCFTR showed that it integrates into an actin-associated, macromolecular complex that includes PDZ domain-containing proteins and ezrin (27, 28). Here, SPT analysis of the dynamics and interactions of rescued ΔF508CFTR revealed novel properties relative to wtCFTR that were related to the peripheral quality control mechanism and, potentially, ΔF508CFTR internalization dynamics.

In live cells at physiological temperature, we found consistently greater cell surface mobility of rΔF508CFTR (by ~30%) compared with wtCFTR, regardless of correction mechanism, which was due to distinct association with PDZ scaffold proteins. Incubation of low temperature-corrected ΔF508CFTR at 37 °C causes increased ubiquitination and endocytosis, and consequent reduced plasma membrane stability (15, 37). Though rΔF508CFTR-PDZ interactions were similar to those of wtCFTR just after low-temperature correction, incubation at 37 °C increased rΔF508CFTR diffusion and reduced PDZ binding. Unfolded ΔF508CFTR is eliminated from the cell surface by the PPQC system. We found that modulation of the PPQC system also altered the diffusion of rΔF508CFTR, suggesting an interdependence of rΔF508CFTR surface stability and mobility.

The role of CFTR-PDZ interactions is incompletely understood. PDZ interactions were initially reported to mediate CFTR polarization, but subsequent contradictory evidence was reported (18, 19). Inconsistent data has also been reported on the role of PDZ interactions in CFTR turnover (19–21). Several studies have concluded that multivalent PDZ scaffolds facilitate compartmentalization of proteins to regulate CFTR activity (17, 38). Our experimental approach provided evidence in live cells for involvement of PDZ interactions in CFTR complexation and stabilization at the cell surface over time scales of minutes. This conclusion is based on experimental approaches that either deleted the PDZ-binding domain from CFTR or used expression of an exogenous peptide (mCh-CFTR-C) to com-

pete with CFTR for PDZ domain-containing scaffold proteins. Previously, knockdown of EBP50 was shown to reduce surface stability of wtCFTR and low-temperature rΔF508CFTR over hours (24). However, interpretation of this study is difficult because EBP50 is a multi-domain protein that interacts with distinct PDZ-binding domain proteins and the actin cytoskeleton. Further, altering EBP50 expression profoundly alters the actin cytoskeleton (26).

In experiments designed to quantitatively relate CFTR diffusion to internalization dynamics in MDCK cells, deletion of the CFTR PDZ-binding domain (~50% increase in diffusion compared with wtCFTR) enhanced endocytosis by ~60% whereas partial disruption of PDZ interactions to mimic rΔF508CFTR diffusion (~30% increase in diffusion) increased internalization by ~30%. Endocytosis of ΔF508CFTR in MDCK cells after low-temperature correction and thermal unfolding, or VX-809 treatment, were ~1.8-fold greater than that of wtCFTR. Therefore, the proportion of rΔF508CFTR internalization that relates to increased rΔF508CFTR diffusion (Fig. 5*D*, *blue dashed line*) could be ~50%. Although reduced scaffold binding and consequent accelerated endocytosis would predispose rΔF508CFTR to lysosomal trafficking and degradation, the overall elimination of rΔF508CFTR is ultimately dependent on channel ubiquitination (14, 15). Indeed, there are several disease-causing CFTRs with C terminus deletions yet relatively mild disease, which has suggested that severe disease, as found for the ΔF508 mutation, requires CFTR structural destabilization and consequent ubiquitination in addition to enhanced endocytosis (14, 15, 19, 21).

A limited number of prior studies have demonstrated that PDZ interactions stabilize proteins at the cell surface by reducing endocytic uptake. For instance, stimulated G-protein coupled receptors that contain PDZ-binding domains segregate into specific clathrin-coated pits to greatly extend their surface lifetime through actin association (39). Similar to the present study, a correlative analysis of protein diffusion and internalization has been performed for the neuronal α-amino-3-hydroxy-5-methyl-4-isoxazolepropionic acid receptor (AMPAR) (40). The AMPAR forms a complex with Stargazin and the PDZ scaffold PSD-95, which result in receptor immobilization at the neuronal postsynaptic density. Disruption of Stargazin-PSD-95 interactions with a cell permeable peptide mimetic of the Stargazin PDZ binding domain increased AMPAR diffusive range by ~1.3-fold and endocytosis by ~4-fold (40). For CFTR, Thelin *et al.* (41) reported that the S13F mutation increased CFTR diffusion coefficient by only ~20%, but increased internalization by ~2-fold. However, in that study CFTR was reported as mobile under control conditions, presumably due CFTR expression at super-physiological levels (27), making interpretation of these findings difficult.

Components of the PPQC network, including CHIP, Hsc70 and Hsp90, were found here to alter the plasma membrane dynamics of rΔF508CFTR after low temperature or chemical correction. Although the mechanism responsible for PPQC modulation of rΔF508CFTR diffusion was not established, we speculate that rΔF508CFTR-PDZ interactions might be reduced by ubiquitination, or perhaps sterically hindered by rΔF508CFTR-CHIP/Hsp90/Hsc70 complex-ation. Further work is required to address these hypotheses. CHIP and associated quality control components have been shown to mediate ubiquination of ΔF508CFTR at the cell surface and the ER, and inhibition of CHIP causes ΔF508CFTR accumulation in the ER (15, 42, 43). Functional inhibition of CHIP or a CHIP-binding partner thus represents a potential therapeutic approach to stabilize rΔF508CFTR at the cell surface.

REFERENCES

1. Rowe, S. M., Miller, S., and Sorscher, E. (2005) Cystic Fibrosis. *N. Engl. J. Med.* **352,** 1992–2001
2. Riordan, J. R. (2008) CFTR function and prospects for therapy. *Annu. Rev. Biochem.* **77,** 701–726
3. Lukacs, G. L., and Verkman, A. S. (2012) CFTR: folding, misfolding and correcting the ΔF508 conformational defect. *Trends Mol. Med.* **18,** 81–91
4. Vembar, S. S., and Brodsky, J. L. (2008) One step at a time: endoplasmic reticulum-associated degradation. *Nat. Rev. Mol. Cell Biol.* **9,** 944–957
5. Denning, G. M., Anderson, M. P., Amara, J. F., Marshall, J., Smith, A. E., and Welsh, M. J. (1992) Processing of mutant cystic fibrosis transmembrane conductance regulator is temperature-sensitive. *Nature* **358,** 761–764
6. Egan, M. E., Glöckner-Pagel, J., Ambrose, C., Cahill, P. A., Pappoe, L., Balamuth, N., Cho, E., Canny, S., Wagner, C. A., Geibel, J., and Caplan, M. J. (2002) Calcium-pump inhibitors induce functional surface expression of ΔF508-CFTR protein in cystic fibrosis epithelial cells. *Nat. Med.* **8,** 485–492
7. Wang, X., Venable, J., LaPointe, P., Hutt, D. M., Koulov, A. V., Coppinger, J., Gurkan, C., Kellner, W., Matteson, J., Plutner, H., Riordan, J. R., Kelly, J. W., Yates, J. R., 3rd, and Balch, W. E. (2006) Hsp90 cochaperone Aha1 downregulation rescues misfolding of CFTR in cystic fibrosis. *Cell* **127,** 803–815
8. Grove, D. E., Rosser, M. F., Ren, H. Y., Naren, A. P., and Cyr, D. M. (2009) Mechanisms for rescue of correctable folding defects in CFTRΔF508. *Mol. Biol. Cell* **20,** 4059–4069
9. Hutt, D. M., Herman, D., Rodrigues, A. P., Noel, S., Pilewski, J. M., Matteson, J., Hoch, B., Kellner, W., Kelly, J. W., Schmidt, A., Thomas, P. G., Matsumura, Y., Skach, W. R., Gentzsch, M., Riordan, J. R., Sorscher, E. J., Okiyoneda, T., Yates, J. R., 3rd, Lukacs, G. L., Frizzell, R. A., Manning, G., Gottesfeld, J. M., and Balch, W. E. (2010) Reduced histone deactylase 7 activity restores function to misfolded CFTR in cystic fibrosis. *Nat. Chem. Biol.* **6,** 25–33
10. Gee, H. Y., Noh, S. H., Tang, B. L., Kim, K. H., and Lee, M. G. (2011) Rescue of ΔF508-CFTR trafficking via a GRASP-dependent unconventional secretion pathway. *Cell* **146,** 746–760
11. Pedemonte, N., Lukacs, G. L., Du, K., Caci, E., Zegarra-Moran, O., Galietta, L. J., and Verkman, A. S. (2005) Small-molecule correctors of defective ΔF508-CFTR cellular processing identified by high-throughput screening. *J. Clin. Invest.* **115,** 2564–2571
12. Van Goor, F., Hadida, S., Grootenhusi, P. D., Burton, B., Stack, J. H., Straley, K. S., Decker, C. J., Miller, M., McCartney, J., Olsen, E. R., Wine, J. J., Frizzell, R. A., Ashlock, M., and Negulescu, P. A. (2011) Correction of F508del-CFTR protein processing defect *in vitro* by investigational drug VX-809. *Proc. Natl. Acad. Sci. U.S.A.* **15,** 18843–18848
13. Phuan, P. W., Yang, B., Knapp, J. M., Wood, A. B., Lukacs, G. L., Kurth, M. J., and Verkman, A. S. (2011) Cyanoquinolines with independent corrector and potentiator activities restore Δphe508-cystic fibrosis transmembrane conductance regulator chloride channel function in cystic fibrosis. *Mol. Pharmacology* **80,** 683–693
14. Sharma, M., Pampinella, F., Nemes, C., Benharouga, M., So, J., Du, K., Bache, K. G., Papsin, B., Zerangue, N., Stenmark, H., and Lukacs, G. L. (2004) Misfolding diverts CFTR from recycling to degradation; quality control at early endosomes. *J. Cell Biol.* **164,** 923–933
15. Okiyoneda, T., Barrière, H., Bagdány, M., Rabeh, W. M., Du, K., Höhfeld, J., Young, J. C., and Lukacs, G. L. (2010) Peripheral protein quality control removes unfolded CFTR from the plasma membrane. *Science* **329,** 805–810
16. Varga, K., Goldstein, R. F., Jurkuvenaite, A., Chen, L.-F., Matalon, S.,

Sorscher, E. J., Bebok, Z., and Collawn, J. F. (2008) Enhanced cell-surface stability of rescued ΔF508 cystic fibrosis transmembrane conductance regulator (CFTR) by pharmacological chaperones. *Biochem. J.* **15,** 555–564
17. Guggino, W. B., and Stanton, B. A. (2006) New insights into cystic fibrosis: molecular switches that regulate CFTR. *Nat. Rev. Mol. Cell Biol.* **7,** 426–436
18. Moyer, B. D., Denton, J., Karlson, K. H., Reynolds, D., Wang, S., Mickle, J. E., Milewski, M., Cutting, G. R., Guggino, W. B., Li, M., and Stanton, B. A. (1999) A PDZ-interacting domain in CFTR is an apical membrane polarization signal. *J. Clin. Invest.* **104,** 1353–1361
19. Benharouga, M., Haardt, M., Kartner, N., and Lukacs, G. L. (2001) COOH-Terminal truncations promote proteasome-dependent degradation of mature cystic fibrosis transmembrane conductance regulator from post-golgi compartments. *J. Cell Biol.* **153,** 957–970
20. Swiatecka-Urban, A., Duhaime, M., Coutermarsh, B., Karlson, K. H., Collawn, J., Milewski, M., Cutting, G. R., Guggino, W. B., Langford, G., and Stanton, B. A. (2002) PDZ domain interaction controls the endocytic recycling of the cystic fibrosis transmembrane conductance regulator. *J. Biol. Chem.* **277,** 40099–40105
21. Haardt, M., Benharouga, M., Lechardeur, D., Kartner, N., and Lukacs, G. L. (1999) C-Terminal truncations destabilize the cystic fibrosis transmembrane conductance regulator without impairing its biogenesis. *J. Biol. Chem.* **274,** 21873–21877
22. Wolde, M., Fellows, A., Cheng, J., Kivenson, A., Coutermarsh, B., Talebian, L., Karlson, K., Piserchio, A., Mierke, D. F., Stanton, B. A., Guggino, W. B., and Madden, D. R. (2007) Targeting CAL as a negative regulator of ΔF508-CFTR cell-surface expression: an RNA interference and structure-based mutagenesis approach. *J. Biol. Chem.* **282,** 8099–8109
23. Cushing, P. R., Vouilleme, L., Pellegrini, M., Boisguerin, P., and Madden, D. R. (2010) A stabilizing influence: CAL PDZ inhibition extends the half-life of ΔF508-CFTR. *Angew Chem. Int. Ed.* **49,** 9907–9911
24. Kwon, S.-H., Pollard, H., and Guggino, W. B. (2007) Knockdown of NHERF1 enhances degradation of temperature rescued ΔF508 CFTR from the cell surface of human airway cells. *Cell Physiol. Biochem.* **20,** 763–772
25. Guerra, L., Fanelli, T., Favia, M., Riccardi, S. M., Busco, G., Cardone, R. A., Carrabino, S., Weinman, E. J., Reshkin, S. J., Conese, M., and Casavola, V. (2005) Na^+/H^+ exchanger regulatory factor isoform 1 overexpression modulates cystic fibrosis transmembrane conductance regulator (CFTR) expression and activity in human airway 16HBE14o- cells and rescues ΔF508 CFTR functional expression in cystic fibrosis cells. *J. Biol. Chem.* **280,** 40925–40933
26. Favia, M., Guerra, L., Fanelli, T., Cardone, R. A., Monterisi, S., Di Sole, F., Castellani, S., Chen, M., Seidler, U., Reshkin, S. J., Conese, M., and Casavola, V. (2010) Na^+/H^+ Exchanger regulatory factor 1 overexpression-dependent increase of cytoskeleton organization is fundamental in the rescue of F508del cystic fibrosis transmembrane conductance regulator in human airway CFBE41o- cells. *Mol. Biol. Cell* **21,** 73–86
27. Haggie, P. M., Kim, J. K., Lukacs, G. L., and Verkman, A. S. (2006) Tracking of quantum dot-labeled CFTR shows near immobilization by C-terminal PDZ interactions. *Mol. Biol. Cell* **17,** 4937–4945
28. Jin, S., Haggie, P. M., and Verkman, A. S. (2007) Single particle tracking of membrane protein diffusion in a potential: Simulation, detection, and application to confined diffusion of CFTR Cl^- channels. *Biophys. J.* **93,** 1079–1088
29. Triller, A., and Choquet, D. (2008) New concepts in synaptic biology derived from single-molecule imaging. *Neuron* **59,** 359–374
30. Haggie, P. M., and Verkman, A. S. (2008) Monomeric CFTR in plasma membranes of live cells revealed by single molecule fluorescence imaging. *J. Biol. Chem.* **283,** 23510–23513
31. Valentine, C. D., and Haggie, P. M. (2011) Confinement of β1- and β2-adrenergic receptors in the plasma membrane of cardiomyocyte-like H9c2 cells is mediated by selective interactions with PDZ domain and A-kinase anchoring proteins but not caveolae. *Mol. Biol. Cell* **22,** 2970–2982
32. Dahan, M., Lévi, S., Luccardini, C., Rostaing, P., Riveau, B., and Triller, A. (2003) Diffusion dynamics of glycine receptors revealed by single-quantum dot tracking. *Science* **302,** 442–445
33. Crane, J. M., and Verkman, A. S. (2008) Long-range nonanomalous diffusion of quantum dot-labeled aquaporin-1 water channels in the cell plasma membrane. *Biophys. J.* **94,** 702–713
34. Clancy, J. P., Rowe, S. M., Accurso, F. J., Aitken, M. L., Amin, R. S., Ashlock, M. A., Ballmann, M., Boyle, M. P., Bronsveld, I., Campbell, P. W., De Boeck, K., Donaldson, S. H., Dorkin, H. L., Dunitz, J. M., Durie, P. R., Jain, M., Leonard, A., McCoy, K. S., Moss, R. B., Pilewski, J. M., Rosenbluth, D. B., Rubenstein, R. C., Schechter, M. S., Botfield, M., Ordoñez, C. L., Spencer-Green, G. T., Vernillet, L., Wisseh, S., Yen, K., Konstan, M. W. (2012) Results of a phase IIa study of VX-809, an investigational CFTR corrector compound, in subjects with cystic fibrosis homozygous for the F508del-CFTR mutation. *Thorax* **67,** 12–18
35. Ballinger, C. A., Connell, P., Wu, Y., Hu, Z., Thompson, L. J., Yin, L. Y., and Patterson, C. (1999) Identification of CHIP, a novel tetratricopeptide repeat-containing protein that interacts with heat shock proteins and negatively regulates chaperone functions. *Mol. Cell Biol.* **19,** 4535–4545
36. Owen, D. M., Williamson, D., Rentero, C., and Gaus, K. (2009) Quantitaive microscopy: protein dynamics and membrane organisation. *Traffic* **10,** 962–971
37. Okiyoneda, T., Apaja, P. M., and Lukacs, G. L. (2011) Protein quality control at the plasma membrane. *Curr. Opin. Cell Biol.* **23,** 483–491
38. Li, C., and Naren, A. P. (2005) Macromolecular complexes of cystic fibrosis transmembrane conductance regulator and its interacting partners. *Pharmacol. Therap.* **108,** 208–223
39. Puthenveedu, M. A., and von Zastrow, M. (2006) Cargo regulates clathrin-coated pit dynamics. *Cell* **127,** 113–124
40. Sainlos, M., Tigaret, C., Poujol, C., Olivier, N. B., Bard, L., Breillat, C., Thiolon, K., Choquet, D., and Imperiali, B. (2011) Biomimetic divalent ligands for the acute disruption of synaptic AMPAR stabilization. *Nat. Chem. Biol.* **7,** 81–91
41. Thelin, W. R., Chen, Y., Gentzsch, M., Kreda, S. M., Sallee, J. L., Scarlett, C. O., Borchers, C. H., Jacobson, K., Stutts, M. J., and Milgram, S. L. (2007) Direct interactions with filamins modulate the stability and plasma membrane expression of CFTR. *J. Clin. Invest.* **117,** 364–374
42. Meacham, G. C., Patterson, C., Zhang, W., Younger, J. M., and Cyr, D. M. (2001) The Hsc70 co-chaperone CHIP targets immature CFTR for proteasomal degradation. *Nat. Cell Biol.* **3,** 100–105
43. Younger, J. M., Chen, L., Ren, H.-Y., Rosser, M. F. N., Turnbull, E. L., Fan, C.-Y., Patterson, C., and Cyr, D. M. (2006) Sequential quality-control checkpoints triage misfolded cystic fibrosis transmembrane conductance regulator. *Cell* **126,** 571–582